Study of martensitic-ferritic dual phase steels produced by hot stamping

E Erişir[1], O G Bilir[1]

[1]Department of Metallurgical and Materials Engineering, Kocaeli University, 41380-Kocaeli-Turkey

corresponding author e-mail address: eerisir@gmail.com

Abstract. The effects of heat treatment and initial microstructure on tensile properties of 22MnB5 and 30MnB5 high-strength hot stamping steels with martensite-ferrite matrix were investigated. Hot stamping steels possessed limited elongations of about 5% in a tensile strength ranging from 1300 to 1500 MPa when quenched at temperatures above A3 temperatures. The total elongations were tried to improve by partial austenization between Ac1 and Ac3 temperature and quenching. Ac1 and Ac3 temperatures were calculated via ThermoCalc. Microstructural characterization was made by using Light Microscope and Scanning Electron Microscope. Microstructure is composed of ferrite+martensite. It was seen that annealing temperature affects the volume fraction of phases. It was concluded that initial microstructure is an important parameter for the final microstructure. This method can be used for automobile parts which require higher TE with sufficient yield and tensile strength. Also this process may be a way of using Zn coated steel sheets in hot stamping process.

1 Introduction

Reducing the fuel consumption without sacrificing the safety properties is only possible with using Ultra High Strength Steels (UHSS) sheets in automotive industry. Dual Phase (DP), Transformation Induced Plasticity (TRIP), Twinning Induced Plasticity (TWIP), Complex Phase (CP) Steels are the most commonly used UHSS. Forming of steel sheets in order to produce body-in-white automobile parts is getting harder as a result of using higher strength steels [1, 2, 3]. Thus, Hot Stamping (HS) process gain importance in recent years by enabling the forming easily to complex geometries without springback or breaking of steel sheets. In HS process, the forming is applied at elevated temperature above Ac3 where the steel sheet has austenitic microstructure. The forming step is followed by quenching in press simultaneously Among other UHSS approaches, HS process gives the highest strength level which is attributed to their fully martensitic microstructure at the end of the process [4]. Market share of hot stamping parts are rising exponentially. There are two important downsides of hot stamped parts. One is that their limited total elongation (TE) behavior. However, TE is not a key necessity in safety zone of an automotive that is responsible of passenger safety. Hot stamped parts are used in safety zones which primarily require high strength. Second drawback of HS is that Zn coated sheet is not suitable for process, because of the Liquid Metal Embrittlement [5].

This study evaluated the extension of the application area of hot stamped parts which require TE in addition to strength. Through-hardened martensitic 22MnB5 and 30MnB5 steels were intercritical annealed at 755 and 775 □C resulting in the formation of dual phase microstructures. It is well

known that Fe diffusion into Zn coating may result with an increased melting temperature for Zn coating as 782°C. Thus, this process may create a potential for galvanized steel sheets to use for hot stamping.

2 Material and Experimental

2.1 Material and Heat Treatment

Hot rolled uncoated commercial 22MnB5 and 26MnB5 steels are used in experimental studies. Detailed chemical compositions of specimens are given in Table 1. First heat treatment was austenitization applied at 945 °C for 15 min. Then, two groups of samples are created by depend on cooling media as air cooled and water quenched. Air cooled 22MnB5, water quenched 22MnB5, air cooled 30MnB5 and water quenched 30MnB5 are called respectively as A, B, C and D. Second heat treatment is applied by partial austenization and water quenching. Partial austenization temperatures are used as 755 and 775°C for 10 min. Critical temperatures are calculated using ThermoCalc [6]. Microstructural characterization was made by using Light Microscope (LM) and Scanning Electron Microscope (SEM). The volume fractions of the microstructural constituents in the dual phase microstructures were measured by phase analysis on a selection of Region Of Interest (ROI) using an image analyzer (OLYMPUS Stream) attached to an LM (OLYMPUS, model: BX41RF-LED) [7].

Table 1. Chemical composition of alloys.

Specimens	Chemical Composition (weight %)							
	C	Si	Mn	P	S	Cr	Mo	Ni
22MnB5	0,237	0,292	1,18	0,0315	0,0064	0,121	<0,0050	0,0370
30MnB5	0,317	0,287	1,15	0,0286	0,0096	0,162	<0,0050	0,0509

In Fig.1, an isopleth diagram showing stability of phases as a function of temperature was given for 0.292 Si, 1.18 Mn, 0.121 Cr, and 0.037 Ni. Volume fraction of austenite and ferrite can be calculated via applying lever rule for related intercritical temperature. The intercritical annealing temperature and the carbon content of alloy both determine the volume fraction of austenite at intercritical range. However, at the same intercritical annealing temperature, carbon content of austenite is the same for steels having different C content. In Fig.1 22MnB5 and 30MnB5 were shown as blue (dotted) and red line respectively. Carbon content of partial austenite for each alloy is also shown as black point. The only difference between 22MnB5 and 30MnB by means of chemical composition is the carbon content. Thus, using the same intercritical temperature for 22MnB5 and 30MnB5, 2 different volume fractions of austenite with same carbon content can be achieved. This could help us to understand th effect of austenite volume fraction for a similar austenite chemical composition.

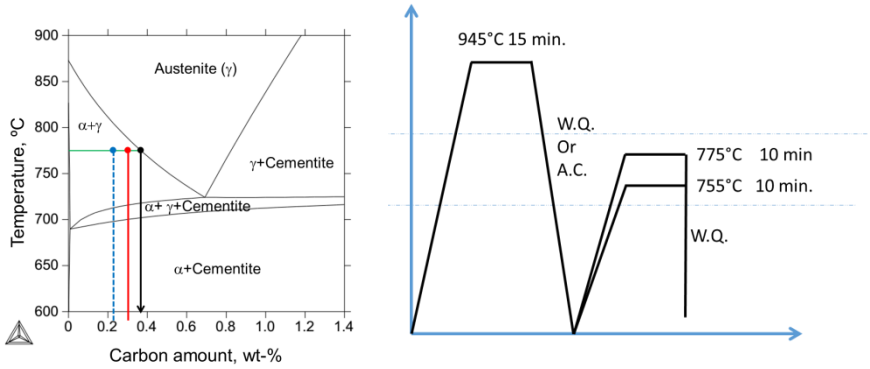

Figure 1. Isopleth diagram and heat treatment steps applied in this study (right). (IA: ıntercritical annealing, W.Q.: Water Quenched, A.C: Air cooled.

2.2 Modeling of Mechanical Properties By Microstructure

It is reasonable to apply rule of mixtures to multiphase steels since each of the micro constituents of steel microstructure show different mechanical properties [8]. According to rule of mixtures, mechanical properties of dual phase steels can be predicted by **equation 1** and **2** given below. Where V_M and V_F are volume fraction of martensite and ferrite. UTS_M, UTS_F and UTS_{DP} are the Ultimate Tensile Strength of martensite and ferrite. TE_M, TE_F and TE_{DP} are the Total Elongation of martensite and ferrite.

$$UTS_{DP}= \{(V_M) \times (UTS_M)\}+\{(V_F) \times (UTS_F)\} \quad (1)$$

$$TE_{DP}= \{(V_M) \times (TE_M)\}+\{(V_F) \times (TE_F)\} \quad (2)$$

Thus, to predict the overall mechanical properties of any dual phase steel one must know the mechanical properties of martensite and ferrite alone. Hot stamped steels are known as fully martensitic steels after the HS operation. Therefore, for low alloyed low carbon steels one can use the mechanical properties of hot stamped steels to predict mechanical properties of martensite alone. If one ignores the additional effect of solid solution strengthening and grain size on mechanical properties for low carbon steel, UTS and TE of martensite may be assumed as 1600MPa and 8% (for optimum values). IF (Interstitial Free) steels are known as single phase ferrite steels. IF steels yield approximately 300MPa of tensile strength with 30% total elongation. As a result, we used mechanical properties of typical IF steel for ferrite. These are the upper limits for commonly used low carbon low alloyed steels without additional treatments. According to Hoofnagel et al. [9] commercial DP600 steels have a volume fraction of 25% martensite while DP800 steels have 41%. Applying proposed model for 25% and 41% volume fraction of martensite resulted with 625 MPa-25% and 833 MPa-21% respectively. These results can be found in mechanical properties of commercial DP600 and DP800 steels.

3 Results and Discussion

In order to evaluate the effect of initial microstructure on dual phase (DP) microstructure, microstructural investigations were performed using SEM and LM. As it can be seen from micrographs in **Fig. 2**, morphology of martensite and ferrite differs depend on initial microstructure. In the intercritical annealing process, austenite may nucleate and grow at different locations depends on initial microstructure [1,2, 10-15]. According to Wei et al. [11] austenite may nucleate at the lath boundaries (LB), packet boundaries (PB) and prior austenite grain boundary (PAGB) during the annealing at the temperature between Ac1 and Ac3. However, a ferrit+pearlite initial microstructure

promotes the nucleation of austenite at pearlite colony boundary, ferrite/cementite interface, and ferrite/ferrite interface [10-15].

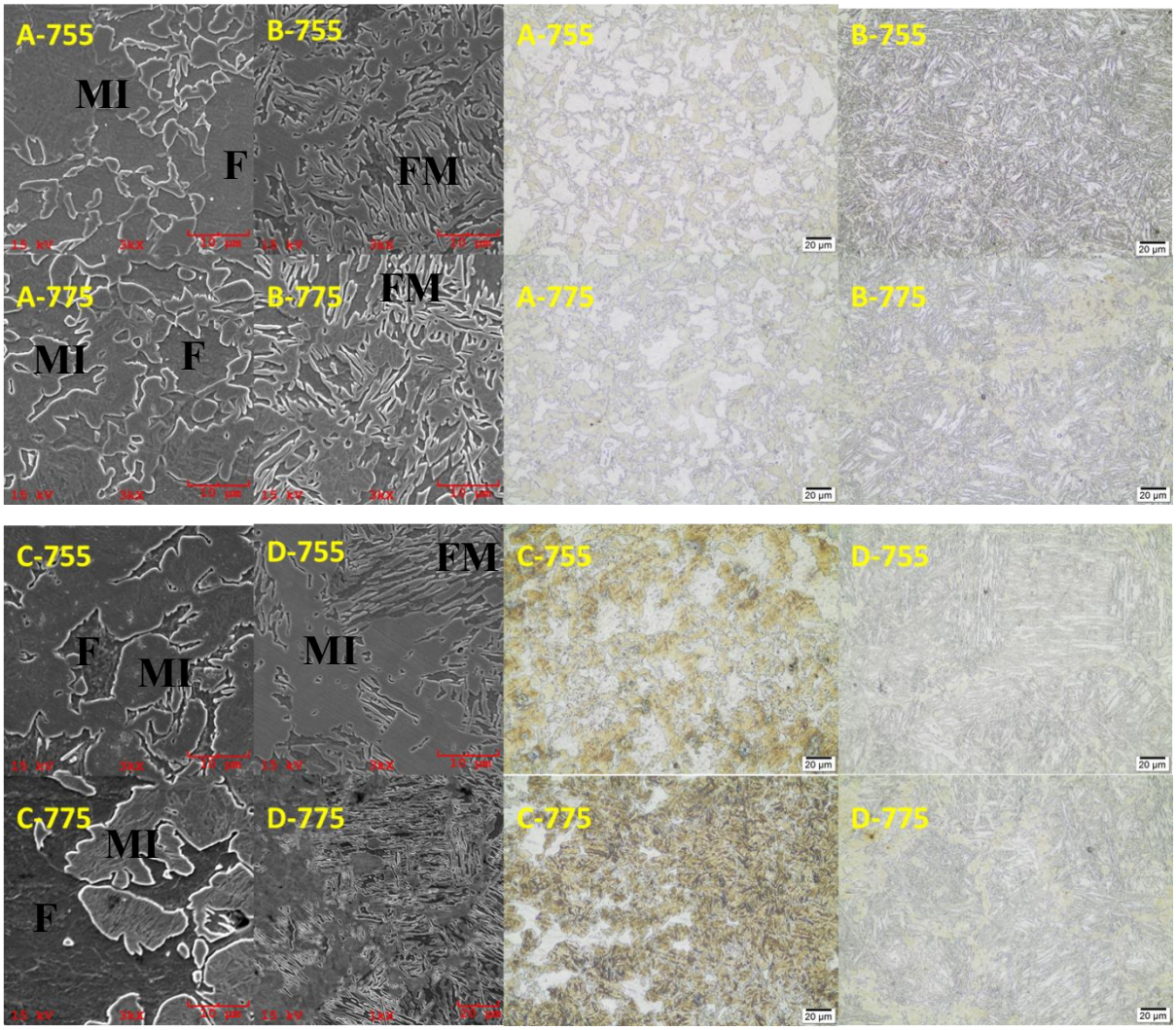

Figure 2. 22MnB5 and 30MnB5 steel with different initial microstructure and partial austenization temperatures. (Air cooled 22MnB5, water quenched 22MnB5, air cooled 30MnB5 and water quenched 30MnB5 are called as A, B, C and D, 755, 775 are intercritical annealing temperature, Darker areas are martensite in light microscope micrographs, MI:Martensite island, FM:Fibrous martensite, F:Ferrite)

Samples B-755, B-775, D-755, D-775 have an initial martensitic microstructure. Thus, DP microstructure mixed of fibrous martensite and ferrite was observed. Fibrous martensite was marked as FM in **Fig2**. In addition to acicular martensite, there are also martensite islands which are coarser and equiaxed. It could be concluded that the formation of different martensite morphologies were due to different nucleation behavior of austenite from initial martensitic microstructure. When an austenite grain nucleates at PAGB or PB, coarse martensite island may be formed. On the other hand, if the nucleation of an austenite grain occurs in LB or PB, it may have finer morphology as martensite fiber. If the initial microstructure is martensite, the transformation of as-quenched martensite to austenite and ferrite can be assumed as a transformation with a single parent phase and two product phases. However, martensite has relatively thin laths and high density

of interfaces compare to coarser ferrite and pearlite constituents [16]. Interfaces are usually considered to be preferred nucleation sites. Moreover, thin laths of martensite represent shorter diffusion distances for carbon, which may control the austenitization process. Samples, A-755, A-775, C-755, C-775 have an initial microstructure of ferrite+pearlite. As shown in **Fig 2**, martensite has granular, coarser and equiaxed morphology. Ferrite was surrounded by martensite islands. Surrounding of ferrite by Blocky type of martensite was also seen by other authors and called as networked morphology [17, 18, 19].Turkmen et al [20] indicated that during quenching from austenite and ferrite region, phase transformation of austenite to martensite may cause deformation of neighbor ferrite phase. Since the networked morphology has less contact surfaces between individual phases than fibrous mixed morphology, it is expected to yield lower strength. Ahmad et al [19] investigated the effect ıf of 3 different initial microstructures as austenite, martensite, ferrite+pearlite on tensile strength. They claimed that coarser martensite and ferrite yielded better tensile and yield strength. It was seen that both raising the carbon content of alloy and intercritical annealing temperature resulted with higher volume fraction of martensite as it is expected. It was also seen that raising the annealing temperature also changed the morphology from fibrous to blocky shaped martensite for the samples have initial microstructure of martensite. Lower volume fraction of fibrous morphology was seen in higher temperatures. It was concluded that at higher annealing temperatures grain growth takes place rather than nucleation of fresh phases due to duration of annealing. To compare the predicted volume fractions of martensite and ferrite phases using Thermocalc, image analysis was conducted in LM images. **Table 2** presents the results acquired from image analysis and thermodynamic calculations. It is apparent that an agreement was obtained between calculated and measured values. Image analyses only applied to samples have initial microstructure of ferrite+pearlite. Proposed model was used to predict mechanical properties of aforementioned samples using the image analysis results.

Table 2. Image Analysis Result and comparison with ThermoCalc

	Measured Values (%) via Image Analysis			**Calculated Values (%) via ThermoCalc**	
Sample	**Ferrite**	**Martensite**	**Deviation**	**Ferrite**	**Martensite**
A-755	49,1	50,9	3,4	44,5	55,5
A-775	25,8	74,2	0,9	29,8	70,2
C-755	26,5	73,5	1,2	29,3	70,7
C-775	11,8	88,2	0,3	11,2	88,8

Sample	**Calculated Mechanical Properties via Proposed Model**			
	Phase Fractions (%)		**Mechanical Properties**	
	Ferrite	**Martensite**	**UTS**	**TE**
A-755	49,1	50,9	961,7	18,802
A-775	25,8	74,2	1264,6	13,676
C-755	26,5	73,5	1255,5	13,83
C-775	11,8	88,2	1446,6	10,596

4 Conclusion

In this study, an alternative to traditional hot stamping process was investigated. Adding ferrite to microstructure beside martensite can be beneficial to have higher elongation. Thus, partial austenitization was carried out rather than full austanization and followed by quenching. It was seen that annealing temperature is proportional to austenite fraction. In partial austenitization process, austenite fraction can be predicted by ThermoCalc. It was seen that thermodynamical calculations were in good agreement with the results of image analysis. According to results, it is possible to have 1000MPa tensile strength with minimum %10 elongation using the heat treatment steps applied in this study. This process may also pave the way for using Zn coated steels in hot stamping.

References

[1] Erişir E and Bilir O G 2016 Effect of Intercritical Annealing Temperature on Martensite and Bainite Start Temperatures After Partial Austenitization. *JOM*, **68(1)** 203-209. doi:10.1007/s11837-015-1673-4
[2] Erişir E Bilir, O G (2014) Effect of intercritical annealing temperature on phase transformations in medium carbon dual phase steels *Journal of materials engineering and performance* ***23*****(3)** 1055-1061.
[3] Calcagnotto M. Adachi Y Pong D Raabe D (2011) Deformation and fracture mechanisms in fine-and ultrafine-grained ferrite/martensite dual-phase steels and the effect of aging. *Acta Materialia* **59(2)** 658-670
[4] Naganathan L. Penter Sheet Metal Forming—Processes and Applications, Chapter 7: Hot Stamping, 2012.
[5] Lee C W Fan D W Sohn I R et al (2012) *Metall and Mat Trans A* **43**: 5122. doi:10.1007/s11661-012-1316-0
[6] Thermodynamic database TCFE6-TCS Steels/Fe-alloys database (v.6.2) for Thermo-Calc, Thermo-Calc SoftwareAB. www.thermocalc.com
[7] http://www.olympus-ims.com/en/microscope/stream2/machinery/
[8] Ahmad E. (2013). Modified Law of Mixture to Describe the Tensile Deformation Behavior of Thermomechanically Processed Dual-Phase Steel. Journal of materials engineering and performance, **22**(8) 2161-2167.
[9] Hoefnagel J P M. et al Experimental and Applied Mechanics, Volume 4: Proceedings of the 2012 Annual Conference on Experimental and Applied Mechanics, Chapter:4
[10] Li Z et al Nucleation of austenite from pearlitic structure in an Fe–0.6C–1Cr alloy (2009) *Scripta Materialia* **60** 485–488,.
[11] Wei R et al (2013) Growth of austenite from as-quenched martensite during intercritical annealing in an Fe–0.1C–3Mn–1.5Si alloy *Acta Materialia* **61** 697–707,
[12] Nakada N et al (2011) Temperature dependence of austenite nucleation behavior from lath martensite *ISIJ International* **51** 299–304.
[13] Shtansky D.V Nakai K Ohmori Y (1999) Pearlite to austenite transformation in an Fe-2.6Cr-1C alloy *Acta Materialia* **47** 2619-2632,.
[14] Savran V.I Leeuwen Y V Hanlon D N Kwakernaak C Sloof W G Sietsma (2007) J Microstructural features of austenite formation in C35 and C45 alloys *Metallurgical and Materials Transactions A* **38** 946–95,.
[15] Savran V I Offerman S E Sietsma J (2010)Austenite nucleation and growth observed on the level of individual grains by three-dimensional x-ray diffraction microscopy, *Metallurgical and Materials Transactions A* **41** 583-591
[16] Esin V. A. et al., In situ synchrotron X-ray diffraction and dilatometric study of austenite formation in a multi-component steel: Influence of initial microstructure and heating rate, Acta Materialia, Vol. 80, 118–131, 2014.
[17] Sarkar, P. P., Kumar, P., Manna, M. K., & Chakraborti, P. C. (2005). Microstructural influence on the electrochemical corrosion behaviour of dual-phase steels in 3.5% NaCl solution. Materials Letters, **59**(19), 2488-2491.
[18] Ahmad, E., Manzoor, T., Ziai, M. M. A., & Hussain, N. (2012). Effect of martensite morphology on tensile deformation of dual-phase steel. Journal of materials engineering and performance, **21**(3), 382-387.
[19] Keleştemur, O., & Yıldız, S. (2009). Effect of various dual-phase heat treatments on the corrosion behavior of reinforcing steel used in the reinforced concrete structures. Construction and building materials, **23**(1), 78-84.
[20] Türkmen, M., & Gündüz, S. (2011). Martensite morphology and strain aging behaviours in intercritically treated low carbon steel. Ironmaking & Steelmaking, **38**(5), 346-352.